The Mediterranean Green Energy Forum 2013, MGEF-13

Performance assessment of different roof integrated photovoltaic modules under Mediterranean Climate

M. D'Orazio[a]*, C. Di Perna[b], E. Di Giuseppe[a]

[a]*Construction, Civil Engineering and Architecture Department, Università Politecnica delle Marche, Ancona 60131, Italy*
[b]*Industrial Engineering and Mathematics Sciences Department, Università Politecnica delle Marche, Ancona 60131, Italy*

Abstract

Many countries, for aesthetic purposes, offer economic advantages (tax deductions, incentives, etc...) for the installation of building integrated photovoltaic modules (BIPV), with water-tightness capability and adequate mechanical resistance in order to substitute tile covering or part of it. Nevertheless, poor or absent ventilation under BIPV panels could cause them to overheat and reduce their efficiency.

It is well established that the presence of an air gap between a photovoltaic (PV) module and roof covering facilitates ventilation cooling under the device and consequently reduces cell temperature and improves its performance.

In this study, we investigated the thermal performance of PV modules installed in a real scale experimental building over a traditional clay tile pitched roof in Italy for almost one year (from August 2009 to June 2010). One PV module was rack-mounted over the roof covering with a 0.2 m air gap; the others were fully integrated and installed at the same level of the roof covering (one with an air gap of 0.04 m, the other mounted directly in contact with the insulation). Temperature and heat flux measurements for each panel, and environmental parameters were recorded.

Experimental results demonstrate that even though the rack-mounted PV module constantly maintains cell temperature below that of the other full-building integrated modules, due to the presence of a higher air gap, the difference in the energy produced by the PV modules estimated for the entire monitoring period is less than 4%.

Keywords: photovoltaic; BIPV; cell temperature; NOCT; Sandia National Laboratory model.

1. Introduction

Some authors recommend high air gaps behind PV modules in order to minimize over-heating and energy loss of the modules, even if there is no clear agreement on optimum gap size for good PV

---

* Corresponding author. Tel.: +390712204587; fax: +390712204582.
E-mail address: m.dorazio@univpm.it.

performance, and values could vary over a wide range. Many studies have investigated the nature of the flow and temperature distribution in air gaps behind PV panels [1], [2], [3],[4]

Nomenclature

T_c	Cell/Module temperature [°C]
T_b	Back-side cell temperature [°C]
T_a	Ambient temperature [°C]
T_r	Reference temperature [°C]
$T_{air\ back}$	Temperature of the air gap behind the module [°C]
k	Ross Coefficient [Km^2/W]
G_t	Total incoming solar radiation [W/m^2]
G_{ref}	Reference solar radiation (1000 W/m^2)
η	Cell/module electrical efficiency [-]
η_r	Cell/module electrical efficiency at temperature Tr [-]
β	Efficiency correction coefficient for temperature [°C-1]
γ	Efficiency correction coefficient for solar irradiance [-]
E	Average daily energy production [kWh]
EP	Average daily energy production related to P [kWh/ kWp]
$\Delta EP_{(A-B)}$	Variation in energy production of module type A in respect to type B [%]
$\Delta EP_{(C-B)}$	Variation in energy production of module type C in respect to type B [%]
P	Peak power [kW]
A	Module surface [m^2]
K	Shading coefficient [-]
η_{bos}	Balance of system efficiency [-]

Gan [5] [6] with the computational fluid dynamics method, determined the effects of air gap size on the thermal performance of PV modules for a range of roof pitches and panel lengths at different solar heat gain levels. He found that a minimum air gap of 0.12-0.15 m is required for multiple module installation and of 0.14-0.16 m for single module installation, depending on roof pitches.

Guiavarch e Peuportier [7] implemented a model for building integrated photovoltaic (BIPV) in a dynamic simulation tool and evaluated the influence of the type of integration of PV collector in buildings on their efficiency. They found out that an air gap of 0.1 m improved the efficiency of PV compared with

the integration without an air gap. However, they defined this difference of efficiency "not dramatic" and underlined that results are to be complemented with architectural and economical aspects.

Recently, many countries, for aesthetic purposes, have started offering economic advantages (tax deductions, incentives, etc...) for the installation of building integrated photovoltaic modules (BIPV). For domestic applications, these kinds of modules often substitute part of the roof covering and are installed totally coplanar to it. The market for these systems is now spreading because they combine electrical production ability with water-tightness, mechanical resistance and poor maintenance.

In Mediterranean countries like Italy, where clay tile roofs are quite diffused, it is normal to have an air gap between 0.03 and 0.06 m directly below the tiles, but at the same time the air gap should not be more than 0.09 m in order to guarantee water-tightness of the roof covering. In these roof mounting configurations, the photovoltaic panels can be installed on the wooden frame of the tiles so as to create small air gaps which are able to cool the modules. Alternatively, the panels can be mounted directly in contact with the insulation. Nevertheless, poor or absent ventilation under the cells could cause an overheating of BIPV, and this especially happens in presence of the current high insulation levels in the building envelope. The consequence could be a reduction in their efficiency.

The aim of this study is to assess the performance of PV mounted on a clay tile roof in three different configurations: rack-mounted over the roof covering, with a minimum air gap between the modules and building envelope and in contact with roof insulation. The research intended to determine whether in a Mediterranean climate, like the one in Italy, it would be necessary to provide higher air gaps on the rear of the panel, as suggested by some researches, in order to minimize overheating and to improve PV performance, or whether the gaps normally provided in traditional configurations of tile roof may be sufficient to ensure good performance.

2. Materials and methods
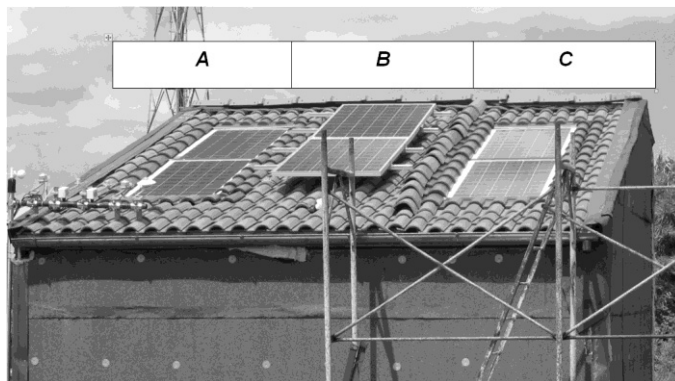
2.1. Experimental devices

Fig. 1 View of the real-scale experimental building with photovoltaic modules,
south pitch (Ancona, Italy).

The research was carried out by analysing the thermal performance and energy efficiency of three PV modules installed on a real-scale experimental building (Fig. 1) near the Marche Polytechnic University of Ancona (Italy, 2064 DD). The roof of the building had a north pitch of 1.5 m and a main south pitch of 6 m and a 17° slope. The latter was divided into 3 roof modules of the same width (1.60 m) and same

length of 5.6 m. The roof systems were all made up of two crossed layers of pine wood panels with a total thickness of 5 cm and EPS insulation of 4 cm. The roofs were different from each other due to the presence of a ventilation duct between the insulation and the traditional clay tile covering (4 cm). The roofs, named A and B, were ventilated, while roof C was not ventilated.

PV modules were installed on the south roof pitch, two panels over each one of the three different roof systems. The modules were made up of mono-crystalline silicon cells (156 x156 mm) and differed from each other by their level of integration, according to Italian law DM 19.02. 2007 [8] in the following way:

- Type A (on roof A): Fully integrated PV module installed at the same level of the roof covering with an air gap of 0.04 m (between the panel and the insulation);
- Type B (on roof B): Partly integrated PV module installed over the roof with an air gap of 0.2 m (between the panel and the tile covering);
- Type C (on roof C): Fully integrated PV module mounted directly in contact with roof insulation.

The modules had a metal frame supporting the cells, which further distanced them from the roof supports (wooden structure for system A, insulation for system C), creating an additional air gap of 0.02 m behind the panels.

2.2. Monitoring system

External weather conditions were recorded throughout almost one year by means of a 12-bit datalogger to which instruments were connected in order to measure global radiation, temperature and relative humidity of the air outside, wind speed and direction. All radiometer probes were arranged on a plane parallel to the pitch plane in order to measure the radiation directly incident on the PV modules.

Internal air temperature and RH% were also measured by a thermal hygrometric probe.

Thermal data on different roofs and modules (Fig. 2) were recorded in the same period by means of 3 12-bit dataloggers connected to:

- thermal resistances for measuring modules front and rear surface temperatures;
- thermal resistances for measuring temperatures within the different layers of the roof (surface of the insulation, air gap, surface of the wood slab);
- heat flow meters for measuring heat flux behind the modules.
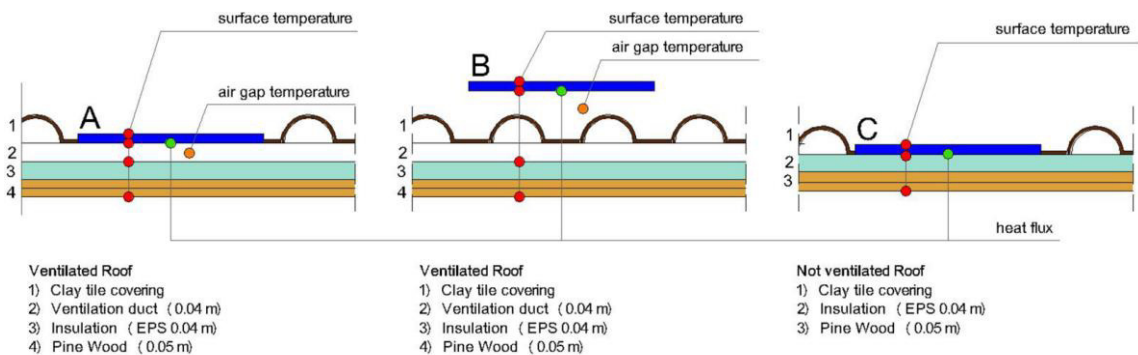

Fig. 2 Position of the probes in the roofs and PV modules. Stratigraphies of the roofs: on the left the ventilated roofs (A, B) and on the right the non-ventilated roof (C).

The accuracy of the probes was +/-0,15°C for PT100 thermal resistances, +/-5% for heat flow meters, $\pm 0.5\%$ of mv for the anemometers, +/-0.1 W/m^2 for radiometric probes, +/- 0.3% for internal and external

air temperature probes, +/- 3% for internal and external RH%.

All the probes and measurement connections were calibrated beforehand, and the calibration results were noted in order to correct the values that were measured. The acquisition rate was set to 10 seconds, while the post processing rate was set to 10 minutes.

2.3. The PV modules temperature and efficiency calculation models

It is actually well established that the temperature of the PV module strongly affects its energy performance. Skoplaki et al. [9] retrieve many correlations which express the adverse effect of an operating temperature increase on the electrical efficiency of the PV module.

As the PV cells are encapsulated for moisture protection, practically cell temperature is very difficult to measure. For major convenience, the temperature at the back of the cell (T_b) is commonly measured instead. The T_b can be obtained from the temperature of the cells (T_c) by the simple expression in (1):

$$T_c = T_b + G_t / G_{ref} \Delta T \qquad (1)$$

In which G_{ref} is the reference solar irradiance (1000 W/m^2), G_t is the total incoming solar radiation (W/m^2), ΔT is the temperature difference between the cell and the back surface of the module at the reference solar irradiance level. This temperature difference is typically 2 to 3 °C for flat-plate modules in an open-rack mount. For flat-plate modules, with a thermally-insulated back surface, this temperature difference can be assumed to be zero.

The simplest explicit equation for the operating temperature of a PV module links T_c with the ambient temperature and the solar radiation flux in a linear expression (2):

$$T_c = T_a + kG_t \qquad (2)$$

Where k is a dimensional parameter, known as Ross coefficient [10], ranging between 0.02-0.04 Km^2/w. Its value depends on the level of integration of the module and the size of air gap behind the modules. Skoplaki et al. [9] adapted the principal k values from data in ref.[11]. Results are listed in Table 1.

Table 1 Principal value of the Ross coefficient k adapted by Skoplaki et al. [9] from data in ref. [11].

PV array type	k (Km^2/W)
Well cooled	0.02
Free standing	0.0208
Flat on roof	0.026
Not so well cooled	0.0342
Transparent PV	0.0455
Façade integrated	0.0538
On sloped roof	0.0563

There are many models for the assessment of photovoltaic module efficiency. The most known is given by the following equation (3), which adjusts the reference module efficiency in standard conditions provided by the manufacturers with the temperature of the cells [12]:

$$\eta = \eta_r [1 - \beta (T_c - T_r) + \gamma \, Log \, G_t] \qquad (3)$$

Most often, the equation is used with γ=0 [13] and then goes down to (4), which represents the

traditional linear expression for the PV electrical efficiency:

$$\eta = \eta_r \left[1 - \beta \left(T_c - T_r \right) \right] \tag{4}$$

Using (4) for each PV module analysed (A,B,C), we could find the effective efficiency (5) and consequently estimate the energy production, as in (6) :

$$\eta_{(A,B,C)} = \eta_r \left[1 - \beta \left(T_{c(A,B,C)} - T_r \right) \right] \tag{5}$$

$$E_{(A,B,C)} = \eta_{(A,B,C)} \cdot \eta_{bos} \cdot A_{(A,B,C)} \cdot G_{(A,B,C)} \cdot K \tag{6}$$

In our case, the module surface areas were 2.43 m^2 for BIPV A and C; 2.92 m^2 for BIPV B. K was equal to 1 because the building was set in an open area and the roof pitch was facing exactly south. $G_{(A,B,C)}$ was directly measured. η_r was 0.133. η_{bos} was considered equal to 0.89. The three PV system modules were formed by a different number of PV cells (for type B 60 cells, while for the types A and C, 50 cells). Therefore, the modules were characterized by different peak powers. In order to compare module performance, it was therefore necessary to relate the energy calculated for each system to its peak power (7):

$$EP_{(A,B,C)} = E_{(A,B,C)} / P_{(A,B,C)} \tag{7}$$

In our case, $P_A = P_C = 0.185$ kWp and $P_B = 0.21$ kWp. Finally we calculated the variation in energy production of module types A and C in respect to type B by the following relations (8,9):

$$\Delta EP_{(A-B)} = (EP_{(A)} - EP_{(B)}) / EP_{(B)} \tag{8}$$

$$\Delta EP_{(C-B)} = (EP_{(C)} - EP_{(B)}) / EP_{(B)} \tag{9}$$

3. Results and discussion

3.1. Experimental and predicted thermal performance of the PV modules

The thermal performance of the PV modules under study was firstly analysed on three summer days with different weather conditions: a sunny day without wind, a cloudy day and a sunny day with wind.

The graphs in Fig. 3, 4, 5 show the weather conditions (air temperature, global radiation) and internal temperature trends recorded during the three days, together with the T_b, the $T_{airback}$, and the heat flux behind the panel.

It can be observed how the partially integrated photovoltaic module B, because of the presence of a high air gap, constantly maintains T_b lower than that of the fully integrated solutions A and C. On a sunny and non-windy day (Fig.3), T_b of module B reached a peak temperature of 65.46°C compared to 77.27 °C of module A and 78.80 °C of module C.

BIPV modules operated at temperatures higher than those of module B, with temperatures ranging from 10 to 15°C above, in agreement with previous researches [14].

In module C, where the structure of the panel remains in contact with roof insulation and the cells are only 0.02 m far from it, the $T_{airback}$ reaches 75.34° C. In module A, where the air gap is wider and more ventilated, the $T_{airback}$ reaches a peak of 60.36°C. The $T_{airback}$ in module B reaches 46.22°C.

The overheating of module C is justified by the limited heat flux behind the panel (maximum 62.54 W/m^2), which is half of the value compared to the values reached in module A (maximum 114.59 W/m^2) and notably lower compared to those in module B (maximum 324.49 W/m^2).

On a sunny windy day (Fig.4), the wind reached a maximum speed of 4.15 m/s (the city of Ancona, where this experimental building is located, is not very windy). A general reduction in T_b was observed in all the PV modules. In particular, the performance of module A improved bringing T_b (peaking at

54.31°C) closer to the maximum values of module B (47.52°C). The T_b in module C, which was only limitedly affected by convection cooling because of the wind, reached a maximum temperature of 64.62 °C.
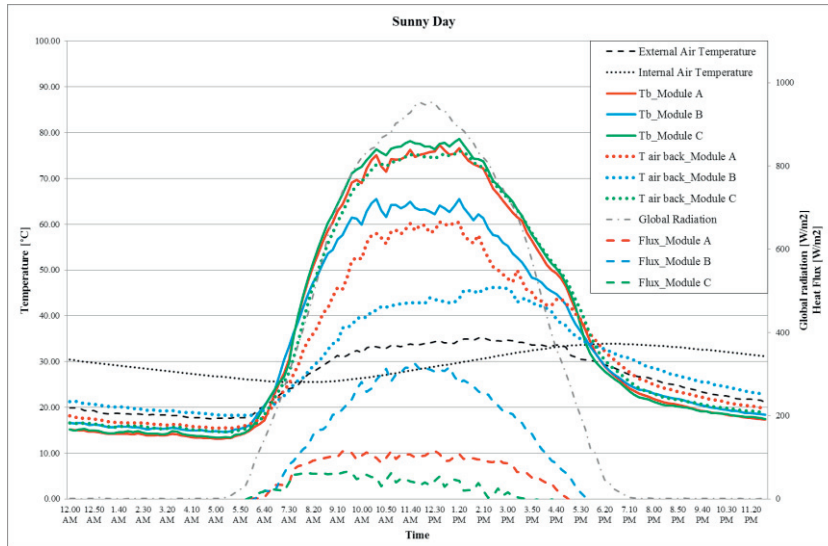

Fig. 3 Sunny and non-windy day (21/08/2009): measured T_b, $T_{airback}$ and heat flux on the PV modules (A, B, C), weather conditions (air temperature, global radiation) and building indoor temperature.
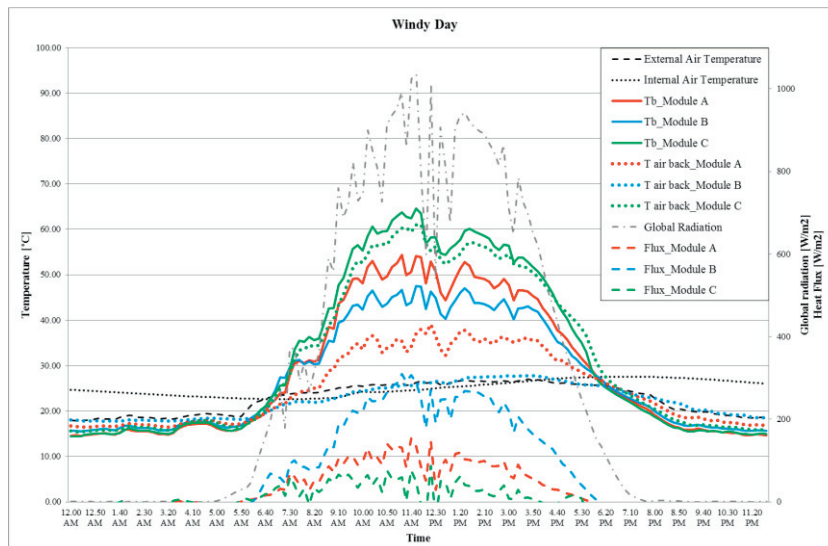

Fig. 4 Sunny and windy day (05/08/2009) : measured T_b, $T_{airback}$ and heat flux on the PV modules (A, B, C), weather conditions (air temperature, global radiation) and building indoor temperature.

In the photovoltaic modules that were ventilated at the back (A and B), there was a substantial reduction in $T_{airback}$ (less than 40° C in module A and less than 30° C in module B), while in module C the

air maintained a temperature close to the temperature at the back of the panel (60,90°C).

In fact, convective heat exchange causes an increase in heat flux at the back of module A even if the air that passes through the air gap between cells and the roof covering is little because of the frictional resistance at the air gap entrance.

On a day with poor solar radiation (Fig.5), the difference in the performance between the three systems levels out substantially. Low solar radiation causes a general lowering of temperature of the panel and of the roof covering.
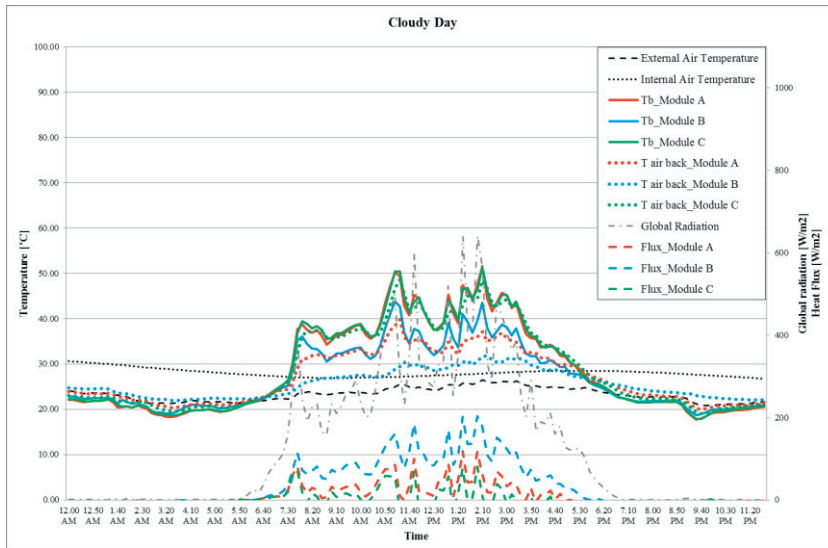

Fig. 5 Cloudy day (30/08/2009): measured T_b, $T_{airback}$ and heat flux on the PV modules (A, B, C),
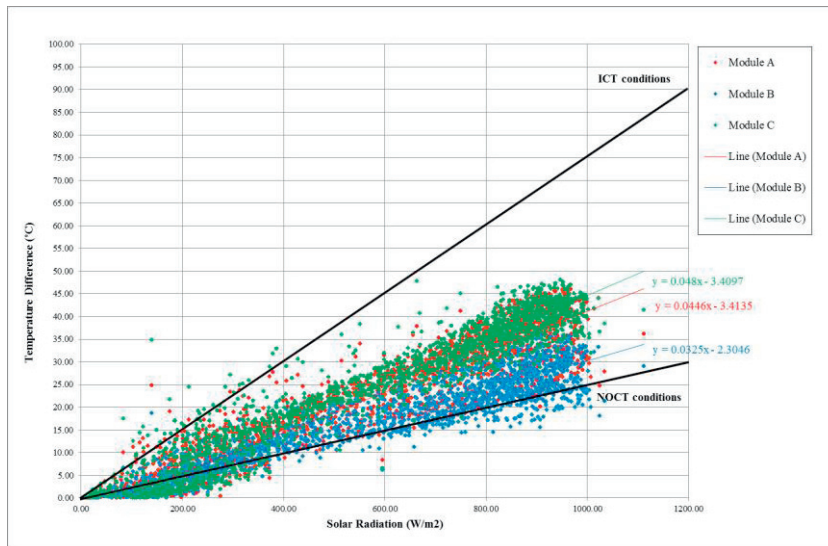weather conditions (air temperature, global radiation) and building indoor temperature.

Fig. 6 PV module and external temperature difference (T_b -T_a) plotted against the solar radiation
for the three modules, throughout the month of August. T_b is experimentally recorded.
Standardized reference lines are given, which show both NOCT and ICT conditions.

The graphs in Fig. 6 show the recorded module and external temperature difference (T_b -T_a) plotted against the solar radiation for the three types of modules, throughout the month of August. Standardized reference lines are given, which show both NOCT and ICT conditions. NOCT (Nominal Operating Cell Temperature) refers to Nominal Terrestrial Environment (NTE) conditions [15]. ICT refers to an Insulated Test Condition (when a module is insulated by 10 cm of expanded polystyrene so that it does not have convective and radiative flow behind it) [16].

The performance of PV modules does not follow a straight line, but something more like a cloud of measurement points due to convective and radiative energy flows, depending on boundary conditions. In general, the large amount of scatter is due to the thermal storage capacity of the panels, the environmental conditions recorded on cloudy days (high external temperatures with low irradiance), and the variations in wind speed.

All the modules analysed show a Ross Coefficient, ranging between 0.029-0.043 Km^2/W, in agreement with the classification by Skoplaki [9]. Module B, which has the lowest T_b, has a Ross coefficient of 0.029 Km^2/W (near the "free standing" mount). The different radiative and convective heat exchanges on the rear side of the BIPV applications A and C cause the trend lines to move upwards: the coefficients of modules A and C are higher and nearer the "not so well cooled" conditions in [9].

3.2. Experimental and predicted yearly energy performance of the PV modules

Annual T_b temperatures actually measured were used to calculate the efficiency of the panels.

In Fig. 7, the average daily energy production given out monthly by the modules have been reported. The graph also show the percentage variation in energy production of module types A and C in respect to type B ($\Delta EP_{(A-B)}$, $\Delta EP_{(C-B)}$).

Experimental results demonstrate that even though the rack-mounted PV module B constantly has a higher energy production, the difference with modules A and C is less than 4%. Module A, with a ventilated air gap, shows a better performance compared to the not ventilated module C: $\Delta EP_{(A-B)}$ is less than 3%.
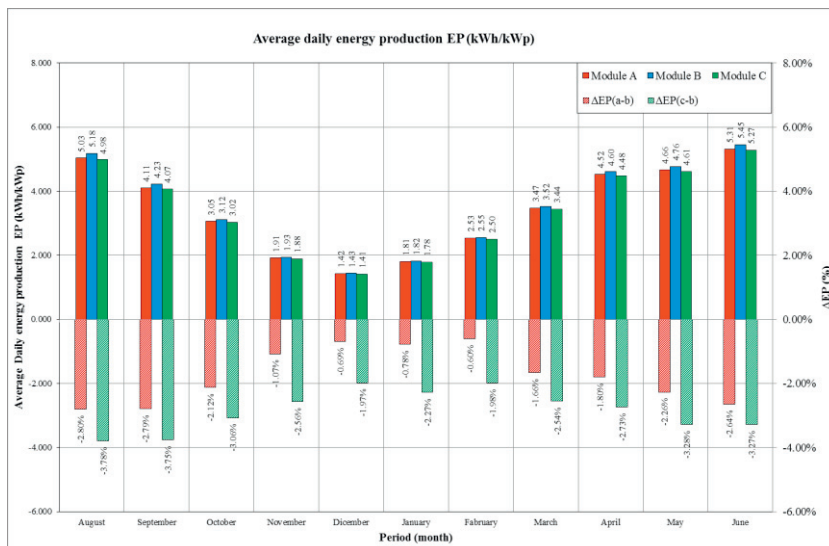

Fig. 7 Average daily energy production values given out monthly by the three PV modules analyzed almost throughout the year (from August 2009 to June 2010).

4. Conclusions

The main conclusions from the investigation of the thermal performance of BIPV modules installed in a real scale experimental building over a traditional clay tile pitched roof in Italy are the following:

- Module B, because of the presence of a high-ventilated air gap, constantly maintains the temperature of the cells lower than that of the fully integrated solutions A and C.
- In BIPV module A, with a ventilated air gap, there is an increased convective heat exchange behind the panel on windy days, with subsequent lowering of cell temperature
- The difference between the energy produced by the three different modules calculated based on the recorded Tb is lower than 4% regardless of installation conditions.

In conclusion, experimental results show that a 0.04 m air gap is enough for reducing the overheating of a BIPV installed on a traditional clay tile roof in Italy. The related energy annual production reaches less than 3% difference with the rack-mounted system.

References

[1] Moshfegh B, Sandberg M, Bloem JJ, Ossenbrink JH. Analysis of fluid flow and heat transfer within the photovoltaic facade on the Elsa building. JRC Ispra, in: Proceedings of the 13th European PV Solar Energy Conference, Nice, 1995: pp. 2215–2217.

[2] Sandberg M, Moshfegh B. Investigation of fluid flow and heat transfer in a vertical channel heated from one side by PV elements—part II, experimental study, in: Proceedings of the World Renewable Energy Conference, 1996: pp. 254–258.

[3] Yang H, Marshall RH, Brinkworth BJ. Validated simulation for thermal regulation of photovoltaic wall structures, in: Proceedings of the 25th IEEE PV Specialists Conference, Washington DC, 1996.

[4] Moshfegh B, Sandberg M. Flow and heat transfer in the air gap behind photovoltaic panels, *Renew. Sust. Energ. Rev* 1998; 2: 287–301.

[5] Gan G. Numerical determination of adequate air gaps for building-integrated photovoltaics, *Sol. Energy* 2009;1–21.

[6] Gan G. Effect of air gap on the performance of building-integrated photovoltaics, *Energy* 2009; 34:913–921.

[7] Guiavarch A, Peuportier B. Photovoltaic collectors efficiency according to their integration in buildings, *Sol. Energy* 2006; 80: 65–77.

[8] DECRETO MINISTERIALE 19 febbraio 2007 Criteri e modalita' per incentivare la produzione di energia elettrica mediante conversione fotovoltaica della fonte solare, in attuazione dell'articolo 7 del decreto legislativo 29 dicembre 2003, n. 387, (in Italian).

[9] Skoplaki E, Palyvos JA. Operating temperature of photovoltaic modules : A survey of pertinent correlations. *Renew. Energ* 2009; 34: 23–29.

[10] Ross RG. Interface design consideration for terrestrial solar cell modules, in: Proceedings of the 12th IEEE Photovoltaic Specialists Conference, Baton Rouge, LA, 1976: pp. 801–806.

[11] Nordmann T, Clavadetscher L. Understanding temperature effects on PV systems performance, in: Proceedings of the Third World Conference on Photovoltaic Energy Conversion, Isaka, Japan, 2003: pp. 2243–2246.

[12] Evans DL. Simplified method for predicting photovoltaic array output, *Sol. Energy* 1981; 27: 555–560.

[13] Evans DL., Cost studies on terrestrial photovoltaic power system with sunlight concentration, *Sol. Energy* 1977; 19: 255–266.

[14] Fuentes MK, A Simplified Thermal Model for Flat-Plate Photovoltaic Arrays, Systems Research. (1987).

[15] ASTM, E 1036M Standard Test Methods for Electrical Performance of Nonconcentrator Terrestrial Photovoltaic Modules and Arrays using Reference Cells, (1999) Vol 12.02.

[16] Bloem GG, Evaluation of a PV-integrated building application in a well-controlled outdoor test environment, *Build. Environ* 2008; 43: 205–216.
.